Colloquium: Looking at a soliton through the prism of optical supercontinuum

Dmitry V. Skryabin* and Andrey V. Gorbach

Department of Physics, Centre for Photonics and Photonic Materials, University of Bath, Bath BA2 7AY, United Kingdom

(Published 29 April 2010)

A traditional view on solitons in optical fibers as robust particlelike structures suited for information transmission has been significantly altered and broadened over the past decade when solitons have been found to play the major role in generation of octave broad supercontinuum spectra in photonic crystal and other types of optical fibers. This remarkable spectral broadening is achieved through complex processes of dispersive radiation being scattered from, emitted, and transformed by solitons. Thus solitons have emerged as the major players in nonlinear frequency conversion in optical fibers. Unexpected analogies of these processes have been found with dynamics of ultracold atoms and ocean waves. This Colloquium focuses on recent understanding and new insights into physics of soliton-radiation interaction and supercontinuum generation.

DOI: 10.1103/RevModPhys.82.1287 PACS number(s): 42.81.Dp, 42.65.Tg, 42.65.Ky, 42.65.Sf

CONTENTS

I. INTRODUCTION

Interplay of dispersion and nonlinear self-action in wave dynamics has been at the focus of attention across many branches of physics since the middle of the past century after the seminal Fermi-Pasta-Ulam work on heat dissipation in solids. This work has been quickly followed by the discovery of many nonlinear wave equations integrable with the inverse scattering technique (IST). Solitons are a particular class of localized and remarkably robust solutions found with the IST technique. Soliton studies have quickly become a subject of its own and have soon developed far beyond the initial subset of integrable models. Localized nonlinear waves in the nonintegrable models are often called solitary waves to distinguish them from IST solitons. However, the use of the original term "soliton" has now widely spread into nonintegrable cases. Solitons have been experimentally observed and studied theoretically in fluid dynamics, mechanical systems, condensed matter, and notably in nonlinear optics. Historic and scientific accounts of these developments can be found, e.g., in Scott (1999).

Optical solitons in fibers (Hasegawa and Tappert, 1973; Mollenauer *et al.*, 1980) have been most extensively researched as potential information carriers (Mollenauer and Gordon, 2006; Agrawal, 2007). With this view in mind solitons can be treated as particlelike objects and their dynamics can be conveniently reduced to the Newton-like equations for the soliton degrees of freedom, such as, e.g., position and phase (Kaup and Newell, 1978; Gorshkov and Ostrovsky, 1981; Mollenauer and Gordon, 2006; Agrawal, 2007). The ability of perturbed solitons to emit dispersive radiation is a property vividly expressing their wave nature. Radiation emission by solitons has been well known in the 20th century (Kivshar and Malomed, 1989; Wai *et al.*, 1990; Karpman, 1993a, 1993b; Akhmediev and Karlsson, 1995), however, it was considered at that time as something that to the large degree undermines usefulness of the soliton concept. This vision has changed dramatically around and after 2000 when the first experimental observation of an octave wide spectral broadening in photonic-crystal fibers was reported by Ranka *et al.* (2000) and subsequently reproduced in dozens of laboratories. This effect has become known as the fiber supercontinuum [see, e.g., Dudley *et al.* (2006), Russell (2006), Knight and Skryabin (2007), and Dudley and Taylor (2009) for recent reviews and Fig. 1]. The above reviews discuss impressive applications of supercontinuum for frequency comb generation in metrology, spectroscopy, and imaging.

After the first experiments on generation of supercontinuum in fibers it has become obvious that solitons are the major players in this process. Spectrally they dominate in the infrared, where the group velocity dispersion (GVD) is typically anomalous. The visible part of supercontinua most often spans through the range of normal

*d.v.skryabin@bath.ac.uk

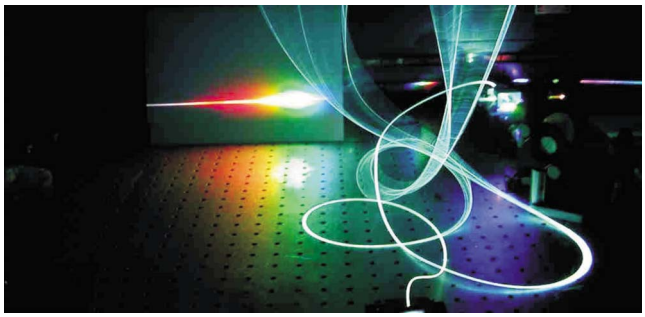

FIG. 1. (Color online) Photograph of supercontinuum generated by an 800 nm femtosecond pulse in a photonic-crystal fiber and projected onto a screen (http://www.bath.ac.uk/physics/groups/cppm/).

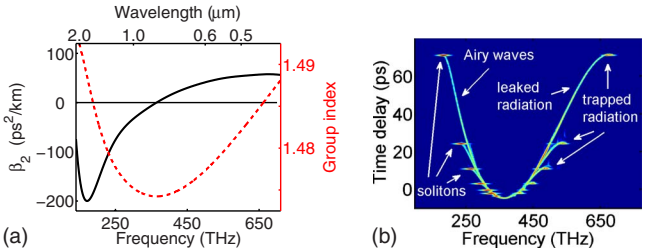

FIG. 2. (Color online) (a) Group index, that is, speed of light divided by the group velocity $n_g = c\partial_\delta k$ (dashed line) and GVD $\beta_2 = \partial_\delta^2 k$ (full line) typical for photonic-crystal fibers used in supercontinuum experiments. The zero GVD point is at $\simeq$790 nm (380 THz) and the normal GVD range is for wavelengths $<$790 nm. (b) XFROG spectrogram showing simultaneous frequency and time-domain pictures of the supercontinuum from Fig. 3 at $z=1.5$ m. Pump wavelength is 850 nm (350 THz).

GVD and is associated with dispersive radiation. Crucially, the dispersive radiation and solitons overlap in the time domain and hence interact by means of the Kerr and Raman nonlinearities.

What was overlooked in the research on fiber solitons in the presupercontinuum era is the fact that interaction of solitons with dispersive waves and the associated frequency conversion processes can be efficient and practically important. Not only experiments but also theory of the soliton-radiation interaction were not developed much beyond the spectrally narrow results following from the integrable nonlinear Schrödinger (NLS) equation, where the solitons are largely insensitive to the interaction with other waves (Zakharov and Shabat, 1972; Kivshar and Malomed, 1989; Kuznetsov *et al.*, 1995). Our primary aims here are to explain the frequency conversion effects resulting from the soliton-radiation interaction and leading to supercontinuum generation in optical fibers and to discuss few other fascinating soliton related effects, which have stem from the supercontinuum research.

II. MODELING OF SUPERCONTINUUM

Talking about supercontinuum generation and soliton-radiation interaction we consider a fiber with sufficiently high nonlinearity and the zero GVD point close to the pump wavelength. These conditions are found in fibers with silica cores of a few ($\sim$1–5 μm) microns in diameter, which can be, e.g., either photonic-crystal or tapered fibers pumped with a variety of sources. The later include femtosecond pulses of mode-locked Ti:sapphire lasers with wavelength around 800 nm (Ranka *et al.*, 2000) and nanosecond pulses from microchip lasers close to 1 μm (Stone and Knight, 2008). An important aspect of the dispersion profile allowing achieving wide supercontinua is the normal GVD extending toward shorter ("bluer") wavelengths [see Fig. 2(a)]. Spectral broadening with the opposite GVD slope has also been studied (Harbold *et al.*, 2002; Efimov *et al.*, 2004).

The widely accepted model well reproducing experimental measurements of supercontinuum is

$$\partial_z A = ik(i\partial_t)A + i\gamma(1-\theta)|A|^2 A + i\gamma\theta A\int_0^\infty dt' R(t')|A(t-t')|^2. \quad (1)$$

Here z is the propagation length and t is the time measured in the reference frame moving with the group velocity at the pump frequency. $\gamma\sim 0.01/\mathrm{W\,m}$ is the nonlinear parameter. $\theta=0.18$ measures the strength of the Raman nonlinearity with respect to the Kerr one and $R(t)$ is the Raman response function (Gorbach *et al.*, 2006; Agrawal, 2007). A is the modal amplitude, which carries all the spectrum we are interested in. $k(i\partial_t)$ is the dispersion operator, usually represented as a polynomial of the order N in $i\partial_t$. The dispersion profile of a linear fiber is recovered by taking $A=e^{ik(\delta)z-i\delta t}$, where $k(\delta)=\Sigma_{n=2}^{N}(1/n!)\beta_n\delta^n$, which is a polynomial fit (not a spectrally local Taylor expansion) of the fiber dispersion. Positive δ's correspond to the absolute frequencies larger than the pump frequency. The GVD coefficient β_2 is calculated as $\beta_2=\partial_\delta^2 k$. $\beta_2=0$ determines location of the zero GVD frequencies.

Equation (1) includes three ingredients: *dispersion* (first term on the right-hand side), *nonlinear phase modulation* due to instantaneous Kerr nonlinearity (second term), and *Raman scattering* (third term). Taken separately these effects are well known. Notably, the last two lead to generation of new spectral content acting on their own. However, conversion into discrete Raman sidebands does not manifest itself in the typical supercontinuum experiments. Also self- (SPM) and cross- (XPM) phase modulations (as particular cases of the generic nonlinear phase modulation) generate spectra, which are relatively narrow (Agrawal, 2007), and cannot explain fully developed supercontinua. It is only when dispersion comes into play and all three of the above effects act together in symphony, then the qualitatively new phenomenon of supercontinuum generation occurs. A typical supercontinuum experiment with the femtosecond 800 nm pump leads to spectra covering range from 400 to 2000 nm after propagation in an $\sim$1-m-long

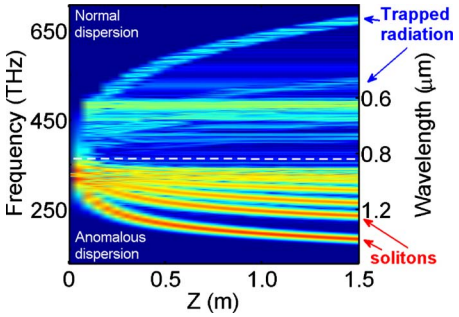

FIG. 3. (Color online) Numerical simulation of supercontinuum generation in a photonic-crystal fiber pumped with 200 fs pulses at 850 nm and having 6 kW peak power. The fiber dispersion as in Fig. 2(a). One can see three stages in the supercontinuum expansion. Symmetric spectral broadening due to SPM happens over first 5 cm. Antisymmetric spectral broadening due to soliton fission accompanied by the emission of the resonant Cherenkov radiation and soliton-radiation interaction both develop between ~5 and ~15 cm. After that the dynamics of the short-wavelength edge is determined by the radiation trapping.

photonic-crystal fiber (Ranka *et al.*, 2000; Wadsworth *et al.*, 2002; Gu *et al.*, 2003). Figures 2(b) and 3 show numerical modeling of this process using Eq. (1).

Results obtained using Eq. (1) have been directly compared with many experimental measurements of femtosecond pulse propagation in photonic-crystal fibers in both time and frequency domains and excellent agreement has been established (Gu *et al.*, 2003; Skryabin *et al.*, 2003; Efimov *et al.*, 2004, 2005, 2006; Gorbach *et al.*, 2006). Probably the most convenient way of representing the data for such comparisons is using the cross-correlation frequency resolved optical gating (XFROG) spectrograms (Gu *et al.*, 2003; Efimov *et al.*, 2004; Hori *et al.*, 2004). The XFROG spectrogram is the Fourier transform of a product of the signal field E with the reference pulse E_r delayed by time τ: $I_{\mathrm{XFROG}}(\tau,\delta)=|\int_{-\infty}^{\infty}E_r(t-\tau)E(t)e^{-it\delta}dt|^2$. E_r is usually a pump pulse and the product of the two fields is generated by the sum frequency process in a $\chi^{(2)}$ crystal.

As with any model, Eq. (1) has limits to its applicability. In particular, it is not applicable to describe sharp field variations occurring over few femtoseconds and less. However, so far the role of such ultrashort features in typical fiber supercontinuum experiments has not been revealed and the octave spectral broadening happens through nonlinear interactions of dispersive waves and solitons which both are well described by Eq. (1). In particular, formation of the coupled soliton-radiation states with the continuously blueshifting radiation component and the redshifting soliton plays a key role in supercontinuum expansion (Gorbach and Skryabin, 2007b, 2007c; Cumberland *et al.*, 2008; Kudlinski and Mussot, 2008; Stone and Knight, 2008; Hill *et al.*, 2009; Travers, 2009).

The relative smoothness of a temporal field profile associated with a typical supercontinuum is one of the reasons why self-steepening (wave breaking) (Agrawal, 2007) does not make notable quantitative and qualitative impacts if included or excluded from Eq. (1). Furthermore, going beyond the amplitude model is likely to be needed for correct description of self-steepening [see, e.g., Amiranashvili *et al.* (2008)]. Therefore we have opted for not taking it into account. In our experience, the most noticeable disagreements of Eq. (1) with the experimental measurements are due to omission of the frequency dependent losses. Other neglected effects are possible excitation of higher order or orthogonally polarized modes, dispersion of the Kerr nonlinearity, third harmonic generation, and noise. Spontaneous Raman noise and input noise are unavoidably present in experiments. The spectra averaged over the statistical ensemble may, in some cases, be better suited for a comparison with measurements, where the fine spectral features of a single pulse excitation can be obscured due to resolution and long (over many pulses) integration time of a spectrum analyzer (Dudley and Coen, 2002; Corwin *et al.*, 2003). Small to moderate pulse to pulse fluctuations in the generated spectra should not prevent us from unraveling and understanding of the deterministic nonlinear processes underlying the supercontinuum generation and the soliton role in it.

III. SOLITON SELF-FREQUENCY SHIFT AND SOLITON DISPERSION

During the first stage of the supercontinuum development SPM induces spectral broadening and associated chirping of a femtosecond pulse (Agrawal, 2007), which are compensated by the anomalous GVD ($\partial_\delta^2 k<0$). Competition of these processes initiates formation of multiple solitons from an initial high power pump pulse (soliton fission) (see Fig. 3). Among the host of the soliton related effects, there are two which are particularly important for us. These are the soliton self-frequency shift induced by the Raman scattering (Mitschke and Mollenauer, 1986) and emission of dispersive radiation. The latter comes from the overlap of the soliton spectrum with the range of frequencies where the fiber GVD is normal (Wai *et al.*, 1990; Karpman, 1993a; Akhmediev and Karlsson, 1995).

Spectra of femtosecond or picosecond solitons are sufficiently narrow, so that the Raman gain profile of silica peaking at 13 THz can be approximated by a straight line rising across the soliton spectrum from the negative values (damping) at the short-wavelength end of the soliton spectrum to the positive values (gain) at the long-wavelength end (Luan *et al.*, 2006; Agrawal, 2007; Gorbach and Skryabin, 2008). The net result on the soliton is that its spectral center of mass is shifted toward redder frequencies (Mitschke and Mollenauer, 1986), which is referred as the soliton self-frequency shift. The group index n_g (ratio of the vacuum speed of light c to the group velocity, $n_g=c\partial_\delta k$) increases with the wavelength providing that the GVD is anomalous. This leads to continuous negative acceleration (deceleration) of solitons by the Raman scattering, which is important for supercontinuum but often forgotten in soliton studies.

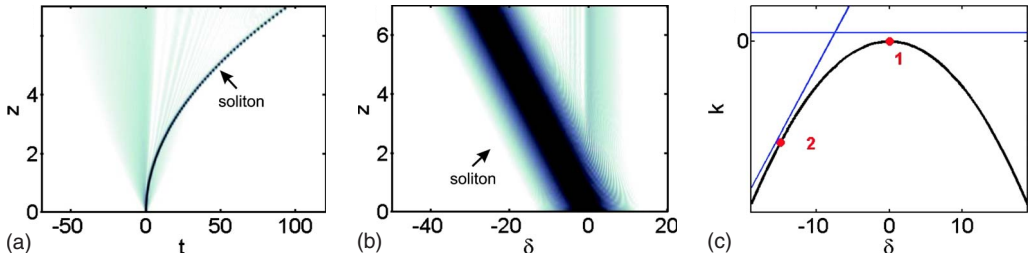

FIG. 4. (Color online) Soliton evolution in (a) (z,t) and (b) (z,δ) planes in the presence of the Raman effect. $k(\delta)=\frac{1}{2}\beta_2\delta^2$. Note that the dispersive waves in (a) are not reflected by the soliton. (c) Phase-matching diagrams between the soliton and dispersive waves [see Eq. (10)]. Straight lines are the soliton wave numbers k_s for two different frequencies δ_s [see Eq. (7)]. Point 1 indicates the initial soliton frequency δ_s and point 2 is δ_s at some distance down the fiber. Parabola shows the dispersion of linear waves $k(\delta)$. All units are dimensionless.

An approximate soliton solution of Eq. (1) moving with a constant acceleration can be derived under the assumption that the fiber group index varies linearly in frequency (i.e., $\partial_\delta k\sim\delta$ and hence $k\sim\delta^2$). For the zero initial frequency, this solution is given by Gagnon and Belanger (1990) and Gorbach and Skryabin (2007a, 2007c),

$$A_s=\psi(t-t_s)\exp[-i\delta_s t+i\phi(z)], \tag{2}$$

$$\psi(t)=\sqrt{2q/\gamma}\,\mathrm{sech}\left(\sqrt{\frac{2q}{|k''|}}t\right), \tag{3}$$

$$\phi(z)=qz+\frac{1}{3}k''\delta_s^2 z,\quad T=\int_0^\infty tR(t)dt, \tag{4}$$

$$\delta_s=\frac{g_0 z}{k''},\quad k''=\partial_\delta^2 k<0,\quad g_0=\frac{32Tq^2}{15}. \tag{5}$$

The soliton delay caused by the Raman effect is $t_s=g_0z^2/2$. $q>0$ is the soliton wave-number shift proportional to its intensity. The soliton trajectory in the (t,z) plane is a parabola given by $t=t_s$ [see Fig. 4(a)]. δ_s is the soliton frequency, which decreases linearly with z [see Fig. 4(b)].

Soliton-radiation interaction discussed below is sensitive to the phase-matching conditions. Therefore it is important to derive spectral representation for an accelerating soliton. The soliton spectrum is calculated as

$$\tilde{A}_s(\delta)=\int_{-\infty}^{\infty}dtA_s e^{i\delta t}=e^{i\phi(z)+it_s[\delta-\delta_s]}\tilde{\psi}(\delta-\delta_s), \tag{6}$$

where $\tilde{\psi}(\delta)=\int_{-\infty}^{\infty}\psi(t)e^{i\delta t}dt$ is a real function. Wave numbers of the soliton spectral components are

$$\begin{aligned}k_s(\delta)&=\partial_z\{\phi(z)+[\delta-\delta_s]t_s\}\\&=q+\partial_\delta k|_{\delta=\delta_s}[\delta-\delta_s]+k(\delta_s).\end{aligned} \tag{7}$$

$k_s(\delta)$ is linear in δ, expressing the fact that the soliton is immune to GVD and hence $\partial_\delta^2 k_s=0$. Also it can be seen that $k_s(\delta)$ is actually a tangent to the dispersion of linear waves $k(\delta)=\frac{1}{2}\beta_2\delta^2$ taken at $\delta=\delta_s$ and shifted away from it by the offset q. If GVD is anomalous for all frequencies ($\beta_2<0$), the soliton spectrum does not touch the spectrum of linear dispersive waves [see Fig. 4(c)].

ψ, as in Eq. (3), is of course an approximate solution, and the Raman effect forces the soliton to shake off some radiation [see Figs. 2(b) and 4(a)]. This radiation can be approximated by Airy functions (Akhmediev *et al.*, 1996; Gorbach and Skryabin, 2008). Airy waves emitted in a typical supercontinuum setting are very weak broad band and have spectrum almost exclusively belonging to the anomalous GVD range. The latter is the main reason why they practically do not interact with solitons and their impact on the supercontinuum spectrum is secondary of importance.

IV. RADIATION EMISSION BY SOLITONS

Solitons dominate the long-wavelength edge of the supercontinuum [see Figs. 1(b) and 2], while the so-called resonant (or "Cherenkov") radiation (Wai *et al.*, 1990; Karpman, 1993a, 1993b; Akhmediev and Karlsson, 1995; Skryabin *et al.*, 2003; Biancalana *et al.*, 2004) comes to mind as one of the reasons for the spectrum created in the normal GVD range (Herrmann *et al.*, 2002; Gu *et al.*, 2003; Cristiani *et al.*, 2004). Despite the importance of the resonant radiation identified in the first efforts to model fiber supercontinuum (Husakou and Herrmann, 2001; Herrmann *et al.*, 2002), later it has become clear that it is only when the initially emitted radiation has a chance to interact with the solitons over long propagation distance, the expanding supercontinua observed in experiments can be reproduced in modeling (Genty, Lehtonen, and Ludvigsen, 2004; Genty *et al.*, 2005; Skryabin and Yulin, 2005; Gorbach and Skryabin, 2007b, 2007c). The Raman effect is the key factor ensuring such interaction.

To model Cherenkov radiation it is often sufficient to include third-order dispersion only, so that a single zero of GVD is taken into account,

$$i\partial_z A-\left(\frac{1}{2!}\beta_2\partial_t^2+\frac{i}{3!}\beta_3\partial_t^3\right)A=-\gamma|A|^2A-T\gamma A\partial_t|A|^2. \tag{8}$$

A linear dispersive solution of Eq. (8) is $A=e^{ikz-i\delta t}$ with $k(\delta)=\frac{1}{2}\beta_2\delta^2+\frac{1}{6}\beta_3\delta^3$. The zero GVD point is located at

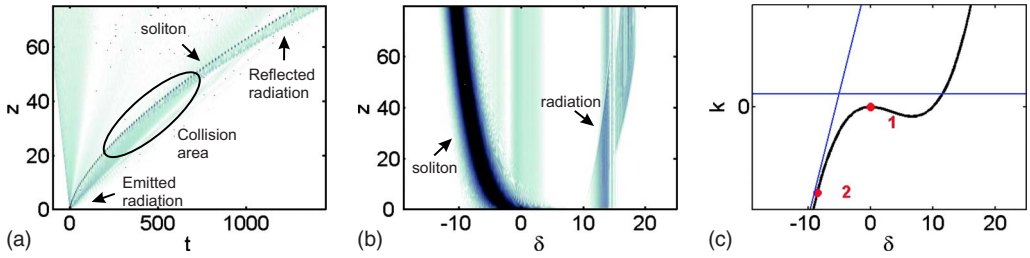

FIG. 5. (Color online) The same as Fig. 4, but with $\beta_3>0$. $k(\delta)=\frac{1}{2}\beta_2\delta^2+\frac{1}{6}\beta_3\delta^3$. Intersections of the straight lines with $k(\delta)$ [see (c)] correspond to the Cherenkov resonances.

$\delta_0=-\beta_2/\beta_3$. The soliton existence condition is $\beta_2<0$ and hence if, e.g., $\beta_3>0$, then the GVD is normal ($\partial_\delta^2 k>0$) toward higher frequencies $\delta>\delta_0$ [see Fig. 5(c)]. The pulse spectrum entering this range is not able to propagate in the soliton regime, which leads to the radiation emission.

Small amplitude Cherenkov radiation F_{Ch} with frequency detuned far from the soliton obeys (Wai *et al.*, 1990; Karpman, 1993a; Akhmediev and Karlsson, 1995; Skryabin *et al.*, 2003; Biancalana *et al.*, 2004)

$$\left(i\partial_z-\frac{1}{2!}\beta_2\partial_t^2-\frac{i}{3!}\beta_3\partial_t^3\right)F_{\mathrm{Ch}}\propto\partial_t^3 A_s. \tag{9}$$

Unlike the above mentioned Airy waves, the resonant radiation is phase-matching dependent and therefore it is narrow band. Using Fourier expansion $F_{\mathrm{Ch}}=\int_{-\infty}^{\infty}\epsilon_{\mathrm{Ch}}(\delta)e^{ik(\delta)z-i\delta t}d\delta$, taking Eq. (6), and calculating z derivatives of the phases involved, we then equate the wave numbers of the left- and right-hand sides of Eq. (9) to find the wave-number matching condition

$$k(\delta)=k_s(\delta). \tag{10}$$

The roots of Eq. (10) are the resonance frequencies δ_{Ch}. $\beta_3>0$ and $\beta_3<0$ gives the blueshiffted and redshifted dispersive waves (see Figs. 5 and 6), respectively. Accounting for the higher-order dispersions is effortless and may lead to several roots of Eq. (10) (Genty, Lehtonen, Ludvigsen, and Kaivola, 2004; Falk *et al.*, 2005; Frosz *et al.*, 2005). The energy of the emitted wave (or waves) is drawn from the entire soliton spectrum resulting in the adiabatic decay of the soliton (Skryabin *et al.*, 2003; Biancalana *et al.*, 2004).

In a typical supercontinuum setting with $\beta_3>0$ the Raman effect increases frequency detuning ($\Delta=\delta_{\mathrm{Ch}}-\delta_s$) between the soliton and its resonance radiation [see Fig. 5(c)]. For $\beta_3<0$ the situation is the opposite [see Fig. 6(c)]. The amplitude of the emitted radiation is proportional to $e^{-a^2|\Delta|}$ (a is a constant), where $\Delta\propto z$ (Wai *et al.*, 1990; Karpman, 1993a; Akhmediev and Karlsson, 1995; Skryabin *et al.*, 2003; Biancalana *et al.*, 2004). Thus for $\beta_3>0$ the soliton self-frequency shift induces an exponential decay of the radiation amplitude with propagation (Biancalana *et al.*, 2004; Gorbach *et al.*, 2006). This implies that the soliton emits significant short-wavelength radiation only at the initial stage of the supercontinuum generation. The radiation emission quickly becomes unnoticeable when the solitons are shifted away from the zero GVD point. Then the natural question is what causes the continuous blueshift of the short-wavelength edge of the supercontinuum (see Fig. 3). The answer is soliton-radiation interaction (not mere radiation emission) (Genty, Lehtonen, and Ludvigsen, 2004; Genty *et al.*, 2005; Gorbach and Skryabin, 2007b, 2007c; Cumberland *et al.*, 2008; Kudlinski and Mussot, 2008; Stone and Knight, 2008; Travers, 2009). The rest of this section and Secs. V and VI elaborate on this in more detail.

If $\beta_3>0$, then the resonant radiation emitted by the soliton has group velocity less than the soliton itself, so that the radiation appears behind the soliton [Fig. 5(a)]. However, after some propagation the radiation catches up with the soliton, which is continuously decelerated by the Raman effect, and the two collide [Figs. 5(a) and 7(a)]. During this collision the radiation is reflected from the soliton backward, and so the next collision becomes unavoidable through the same mechanism. The process can be repeated many times (see Fig. 7). Note that the radiation colliding with the soliton should not be neces-

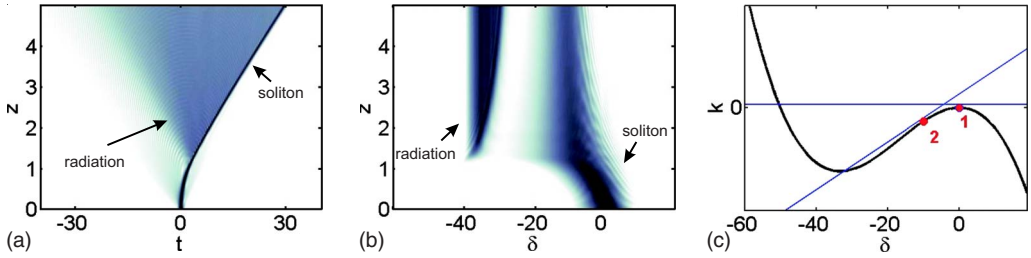

FIG. 6. (Color online) The same as Fig. 4 but with $\beta_3<0$. $k(\delta)=\frac{1}{2}\beta_2\delta^2+\frac{1}{6}\beta_3\delta^3$. Intersections of the straight lines with $k(\delta)$ [see (c)] correspond to the Cherenkov resonances.

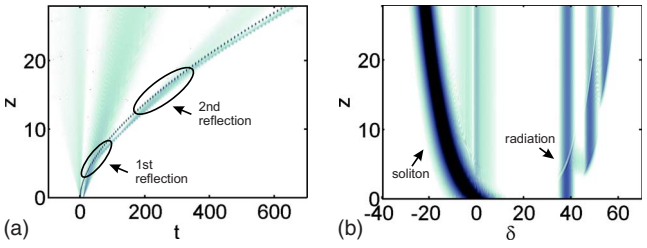

FIG. 7. (Color online) A weak Gaussian pulse in normal GVD range initially placed behind the soliton experiences multiple reflections from the latter. After each collision some light gets through the soliton and some is reflected back. The reflected light is localized close to the soliton and almost indistinguishable from it in the (z,t) plot (a). However, the reflected light is clearly visible in the spectral (z,δ) plot (b) because its frequency is blueshifted after each collision.

sarily emitted by the soliton itself; it can be initiated by other mechanisms, e.g., via SPM or emitted by other solitons (Figs. 7 and 8). An important condition for the reflection of radiation from a soliton to actually happen is that the radiation frequency should belong to the normal GVD range. Radiation in the anomalous GVD range practically does not see solitons since the model is close to the ideal integrable NLS.

Reflection of radiation backward (toward smaller z and larger t) from the soliton implies that the radiation group velocity is further reduced; i.e., the group index $\partial_\delta k$ for the radiation increases. For the normal GVD ($\partial_\delta^2 k>0$) the increase in the group index occurs simultaneously with the increase in frequency δ. Therefore the backward reflections have to be accompanied by blue-

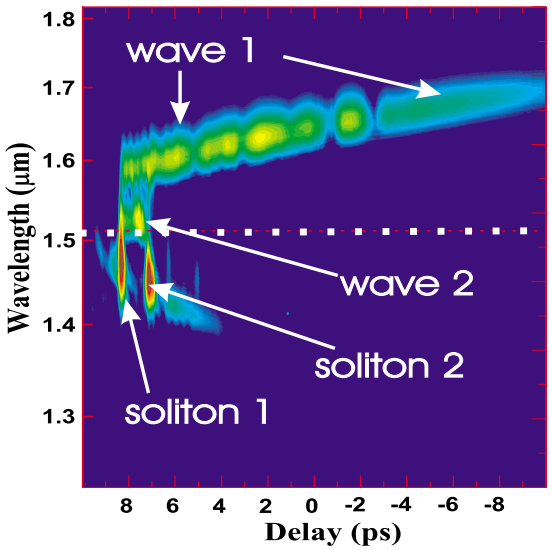

FIG. 8. (Color online) Experimentally measured XFROG spectrogram showing emission of the strong long-wavelength radiation and its reflection from the second soliton in a fiber with $\beta_3<0$ (Efimov *et al.*, 2004). The strong resonant radiation (wave 1) is emitted by the soliton 1. The weaker soliton 2 reflects a part of this wave backward and simultaneously transforms frequency of the reflected radiation (wave 2). Dotted line marks the zero GVD wavelength.

shifting of the radiation frequency [see Fig. 7(b)]. This is exactly the type of process happening between the solitons and short-wavelength radiation in the expanding supercontinuum shown in Fig. 3 (Gorbach *et al.*, 2006; Gorbach and Skryabin, 2007b, 2007c). Obviously the reflection process is nonlinear in its nature, which is explained in detail in Sec. V.

For $\beta_3<0$, the detuning between radiation and the soliton reduces with propagation [Fig. 6(c)], therefore radiation is exponentially amplified in z. This amplification leads to the strong spectral recoil on the soliton followed by the compensation of the soliton self-frequency shift (Skryabin *et al.*, 2003; Biancalana *et al.*, 2004; Efimov *et al.*, 2004; Tsoy and deSterke, 2006) [see Fig. 6(b)]. In this case radiation is emitted ahead of the soliton and has no chance of interacting with it [see Fig. 6(a)]. Radiation can, however, interact with other solitons present in the fibers, bounce back from them, and has its frequency transformed (Efimov *et al.*, 2004; Gorbach and Skryabin, 2007c) (see Fig. 8).

We also note that dark solitons existing for the normal GVD are known to emit Cherenkov radiation into the anomalous GVD range (Karpman, 1993b; Afanasjev *et al.*, 1996). Amplification of this radiation by the Raman effect and its possible use for generation of broad continua has recently been investigated (Milián *et al.*, 2009).

V. SCATTERING OF RADIATION FROM SOLITONS AND SUPERCONTINUUM

In its essence the scattering of a dispersive wave from a soliton is a four-wave mixing (FWM) nonlinear process sensitive to the phase-matching conditions (Efimov *et al.*, 2004, 2005, 2006; Yulin *et al.*, 2004; Skryabin and Yulin, 2005; Gorbach *et al.*, 2006). The latter, however, work out in an unusual way. An important difference of the soliton-radiation interaction with four-wave mixing of dispersive waves only (Agrawal, 2007) is that one of the participating fields is a nondispersing pulse (soliton) having straight-line dispersion and moving with a group (not phase) velocity [see Eq. (7)].

Assume that F_p and δ_p are the amplitude and frequency of the dispersive wave incident on the soliton A_s, while F is the reflected signal field with an unknown frequency δ. The equation for F is (Skryabin and Yulin, 2005)

$$\left(i\partial_z-\frac{1}{2!}\beta_2\partial_t^2-\frac{i}{3!}\beta_3\partial_t^3\right)F=-\gamma|A_s|^2F_p-\gamma A_s^2F_p^*. \quad (11)$$

Thus F is excited by $|A_s|^2F_p$ and $A_s^2F_p^*$ with relative efficiency of the two excitation channels determined by the phase matching. Assuming that the incident wave is $F_p=\epsilon_p e^{ik(\delta_p)-i\delta_p t}$ and using Eqs. (2)–(7), we find the spectral content of the FWM terms,

$$|A_s|^2F_p=\epsilon_p e^{ik(\delta_p)z}\int_{-\infty}^{\infty}f(\delta-\delta_p)e^{it_s[\delta-\delta_p]-i\delta t}d\delta, \quad (12)$$

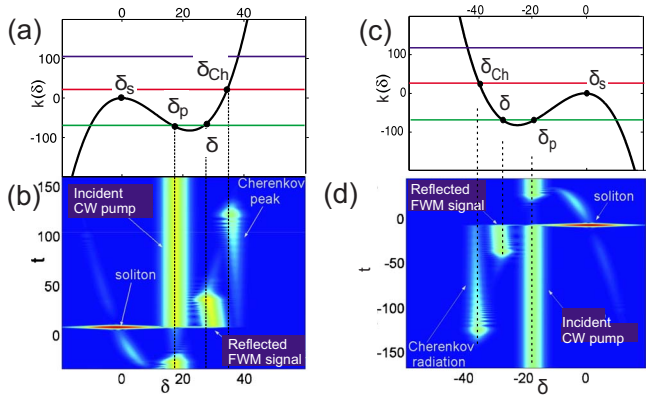

FIG. 9. (Color online) Scattering of radiation from a soliton. (a) and (c) Wave number matching diagrams and (b) and (d) XFROG spectrograms for the fiber pumped with the soliton and cw (Raman effect is disregarded). (a) and (b) $\beta_3>0$ and (c) and (d) $\beta_3<0$. The black curved lines in (a) and (c) are $k=\beta_2\delta^2/2+\beta_3\delta^3/6$. The upper and lower horizontal lines in (a) and (c) correspond to the FWM resonances given by Eqs. (14) and (15), respectively. The middle horizontal lines in (a) and (c) give Cherenkov resonances [Eq. (10)].

$$A_s^2F_p^* = \epsilon_p^* e^{2i\phi(z)-ik(\delta_p)z} \times \int_{-\infty}^{\infty} f(\delta+\delta_p-2\delta_s)e^{it_s[\delta+\delta_p-2\delta_s]-i\delta t}d\delta, \quad (13)$$

where $f(\delta)=\int_{-\infty}^{\infty}\psi^2(t)e^{i\delta t}dt$.

Using (a) Fourier expansion $F=\int_{-\infty}^{\infty}\epsilon(\delta)e^{ik(\delta)z-i\delta t}d\delta$ and taking z derivatives of the phases involved [cf. Eq. (7)] we equal the wave number of F to the wave numbers of Eqs. (12) and (13). The results are (Efimov *et al.*, 2004, 2005, 2006; Yulin *et al.*, 2004; Skryabin and Yulin, 2005; Gorbach *et al.*, 2006)

$$k(\delta) = k_s(\delta) - [k_s(\delta_p) - k(\delta_p)], \quad (14)$$

$$k(\delta) = k_s(\delta) + [k_s(\delta_p) - k(\delta_p)]. \quad (15)$$

Here k is the wave number of the generated wave. $k_s(\delta)$ and $k_s(\delta_p)$ are the soliton wave numbers at the generated frequency and at the frequency of the wave incident on the soliton, respectively. For $\delta_s=0$, $k_s(\delta)=q$ and Eqs. (14) and (15) are simplified to $k(\delta)=k(\delta_p)$, $k(\delta)=2q-k(\delta_p)$.

Solving Eqs. (14) and (15) graphically we find that they predict up to four resonances [see Figs. 9(a) and 9(c)] (Skryabin and Yulin, 2005). One resonance is obvious, $\delta=\delta_p$, and coincides with the frequency of the incident wave (cw pump). The $|A_s|^2F_p$ term and Eq. (14) are responsible for two nontrivial resonances falling into the regions of normal and anomalous GVDs. The former one is typically much stronger and corresponds to the reflection of the wave from the soliton potential. The remaining one and the resonance predicted by Eq. (15) usually do not scatter much of the incident wave and produce weak but detectable signals. Figures 9(a) and 9(b) show the case when the incident wave is reflected backward from the soliton with simultaneous upshift of the reflected wave frequency. Figures 9(c) and 9(d) show the case when the radiation-soliton collision happens at the front edge of the soliton and the wave is reflected ahead of the soliton. The frequency is down-shifted in the latter example.

Equations (14) and (15) apply without a change if the soliton and dispersive waves are orthogonally polarized, which has been used in the experimental measurements of the soliton-radiation interaction (Efimov *et al.*, 2005, 2006). These measurements fully confirmed the validity of both Eq. (14) (Efimov *et al.*, 2005) and Eq. (15) (Efimov *et al.*, 2006). Corresponding examples of the experimental XFROG spectrograms are shown in Fig. 10.

It has been verified that the frequency upshift of the radiation, resulting from the cascaded back reflection of radiation from intensity of the accelerating soliton $|A_s|^2$, is the mechanism ensuring (a) blueshift of the short-wavelength edge of the supercontinuum (Gorbach *et al.*,

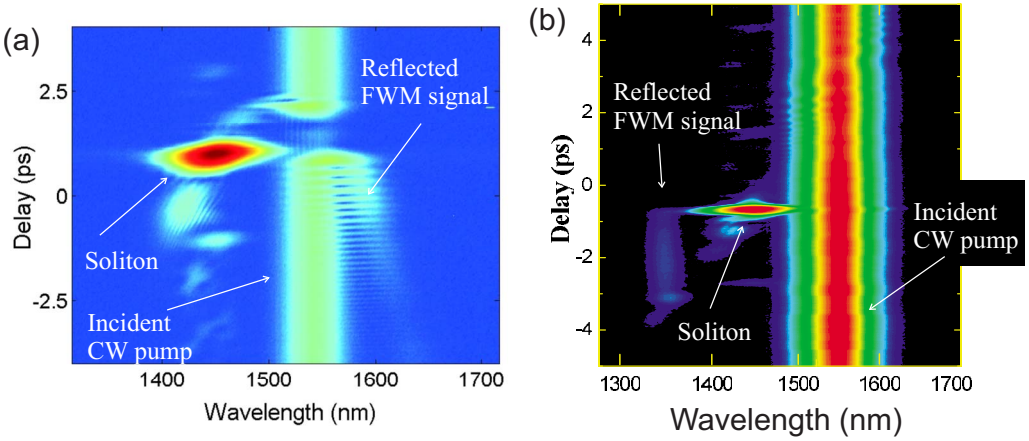

FIG. 10. (Color online) Experimentally measured XFROG spectrograms showing the radiation-soliton interaction. (a) The resonance given by Eq. (14) (Efimov *et al.*, 2005) and (b) given by Eq. (15) (Efimov *et al.*, 2006). (a) The case of the forward reflected wave as in Fig. 9(d). Both (a) and (b) measurements have been taken for $\beta_3<0$.

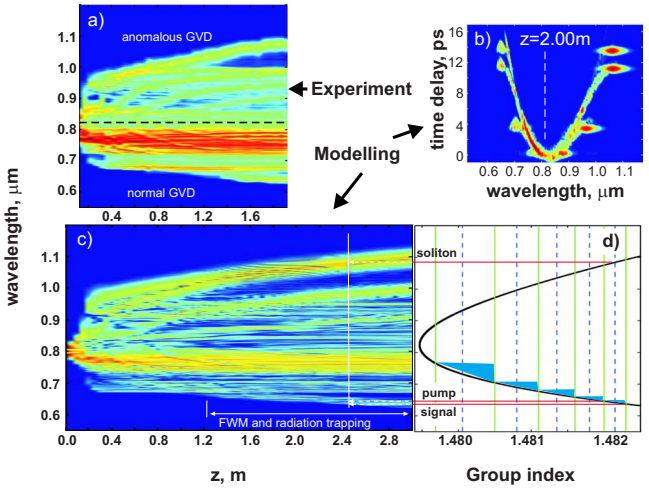

FIG. 11. (Color online) Spectral evolution along the fiber length. (a) Experiment and (c) modeling. (b) XFROG diagram computed for the propagation distance $z=2$ m. (d) Group index as a function of wavelength. The decrease in height of the shaded triangles shows the decreasing frequency difference between the incident and reflected waves (Gorbach *et al.*, 2006).

2006). The phase matching condition (14) works out in a way that with every reflection the frequencies of the incident and reflected waves both tend toward the limit point, where the group velocity of the dispersive wave coincides with the soliton group velocity (Skryabin and Yulin, 2005; Gorbach *et al.*, 2006) (see Fig. 11). Indeed, if the instantaneous soliton frequency is assumed to be zero, then the minimum of $k(\delta)$ corresponds to the frequency with the group velocity matched to the soliton group velocity [Fig. 9(a)]. If the frequency of the incident wave (δ_p) is exactly at this minimum or very close to it, then the resonance predicted by Eq. (14) is either degenerate or close to the degeneracy with δ_p. Under such conditions the process of frequency conversion occurs within a single wave packet and can be termed as the intrapulse four-wave mixing (Gorbach *et al.*, 2006).

In the above picture of the soliton-radiation interaction, it remains unclear what sustains the efficiency of the process over long propagation distances. Strong normal GVD acting on the dispersive wave packet should lead to its sufficiently fast spreading and drop in the peak intensity terminating any nonlinear interaction. Instead, as originally measured by Hori *et al.* (2004) and can be seen from the modeling results [Figs. 3(b) and 11(b)], the wave packets on the short-wavelength edge of the continuum remain localized on the femtosecond time scale and propagate in the solitonlike regime albeit in the normal GVD range. This problem is addressed in Sec. VI.

VI. RADIATION TRAPPING AND SUPERCONTINUUM

What stops dispersive spreading of the radiation wave packets at the short-wavelength edge of supercontinuum and keeps them localized on the femtosecond time scale? The short answer is the refractive index change created by the decelerated soliton exerts a special type of inertial force and ensures dispersionless propagation (trapping) of the radiation.

Reflection of radiation from a soliton plays the major role in the trapping mechanism. Mathematically this is described by Eq. (11) with the first nonlinear term on the right-hand side (see Sec. V). Switching into the reference frame moving together with the soliton reveals two distinct propagation regimes. If the offset of group velocities of the soliton and radiation is sufficiently large and the fiber length is relatively short, then the reflection from the soliton of course occurs, but recurrent collisions leading to trapping can be disregarded (Skryabin and Yulin, 2005). The trapping phenomenon becomes the dominant feature of the propagation when group velocities of the soliton and radiation are sufficiently close (Gorbach and Skryabin, 2007a, 2007b, 2007c; Stone and Knight, 2008; Hill *et al.*, 2009; Travers and Taylor, 2009).

Formal consideration of the problem starts from Eq. (11) complemented by the equation for the soliton field. We choose the reference frequencies of the soliton (δ_s) and radiation (δ_p) so that the group velocities are matched $[k'(\delta_s)=k'(\delta_p)]$ across the zero GVD point and assume

$$E = A_s \exp[ik(\delta_s)z - i\delta_s t] + F \exp[ik(\delta_p)z - i\delta_p t]. \tag{16}$$

For the amplitudes $A_s(z,t)$ and $F(z,t)$ we make substitutions (Gorbach and Skryabin, 2007b, 2007c),

$$A_s = \psi(z,\xi)\exp\left[-it\frac{gz}{k_s''} + iqz + \frac{1}{3k_s''}g^2z^3\right], \tag{17}$$

$$F = \phi(z,\xi)\exp\left[-it\frac{gz}{k_p''} + i\lambda z + \frac{1}{3k_p''}g^2z^3\right], \tag{18}$$

$t_s=gz^2/2$, $\xi=t-t_s$, $k''_{s,p}=\partial_\delta^2 k(\delta_{s,p})$.

We have introduced the g parameter to indicate that the deceleration rate for the soliton interacting with radiation can be different from g_0 for a pure soliton [see Eq. (5)]. GVD for the soliton and radiation are anomalous ($k_s''<0$) and normal ($k_p''>0$), respectively. Thus the directions of the frequency shifts acquired by the two waves are opposite [see the first terms in the exponential factors of Eqs. (17) and (18)]. The group indices felt by the soliton and radiation ($\partial_z t_s=gz$) increase with the same rate (see also discussion in Sec. V) and hence they experience equal negative acceleration.

Now our problem is reduced to a formal question: Is there a solution for ϕ retaining its localized form? In order to answer this formally we substitute Eqs. (16)–(18) into Eq. (1) and neglect several small terms, including the ones nonlinear in the radiation amplitude $|\phi|^2$ (Gorbach and Skryabin, 2007c). Then, the z independent, i.e., shape preserving, radiation waves have to satisfy

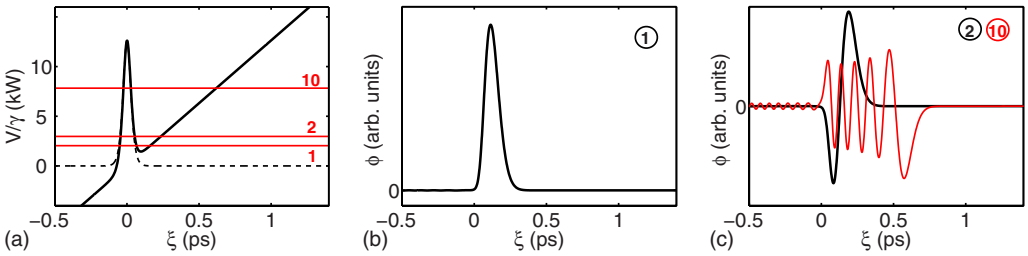

FIG. 12. (Color online) Trapping potential and quasibound radiation modes. (a) Full line shows the potential V. The dashed line shows the potential with the contribution from the inertial force disregarded, which removes the minimum and makes the radiation trapping impossible. Level lines indicate ground state, second, and tenth modes. (b) The ground state mode of the potential V and (c) The second and tenth modes.

$$-\frac{1}{2}k_p''\partial_\xi^2\phi_n+2\gamma|\psi|^2\phi_n+\frac{g\xi}{k_p''}\phi_n=\lambda_n\phi_n,\quad k_p''>0. \tag{19}$$

The above is the linear Schrödinger equation with the effective potential energy $V=2\gamma|\psi|^2+g\xi/k_p''$. The first term inside V is the repelling potential created by the refractive index change induced by the soliton. The dispersive wave reflects from it, as described in Sec. V. The second term in V is the potential linearly increasing in ξ, which exists only due to the fact that we have switched into the noninertial frame of reference accelerating together with the soliton. Hence this term represents a type of inertial force acting on photons. It is known from classical mechanics that inertial forces act as usual ones but show up in the equations of motion only when an appropriate noninertial frame of reference is introduced.

Overall the potential $V(\xi)$ has a well-defined minimum and therefore supports quasilocalized modes (bound states) (see Fig. 12). These modes can be found either numerically or using a variational approach (Gorbach and Skryabin, 2007c). Taking the soliton plus one of these modes and substituting them into Eqs. (17) and (18) result in the spectral evolution shown in Fig. 13. The soliton spectrum moves continuously to the smaller frequencies and the radiation spectrum moves toward higher frequencies. The sign of β_3 is implicit but important here. If $\beta_3>0$, as in the typical supercontinuum generation experiments, then initially $\delta_s<\delta_p$ and the soliton and radiation spectrally diverge with propagation. However, if $\beta_3<0$, then $\delta_s>\delta_p$, while the spectral shifts still act in the same directions, so that frequencies of the soliton and radiation converge with propagation (Gorbach and Skryabin, 2007c).

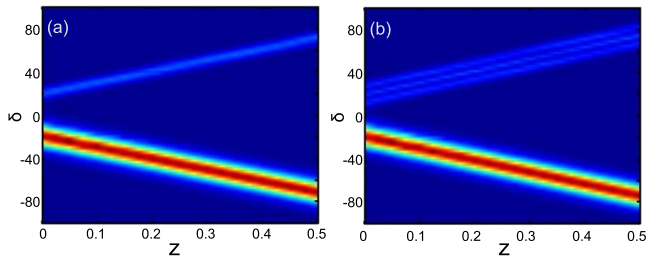

FIG. 13. (Color online) Spectral evolution of the soliton-radiation bound states with (a) $n=1$ and (b) $n=3$ given by Eqs. (17) and (18).

One can notice that taking the higher-order modes leads to temporal [Fig. 12(c)] and spectral (Fig. 13) broadening of radiation. Spectral trajectories in Fig. 13 follow the straight lines because Eqs. (17) and (18) assume frequency-independent GVD. In a real fiber the soliton and radiation moving away from the zero GVD point encounter increasing absolute values of the GVD. This leads to the adiabatic broadening of the soliton and reduces its Raman shift [Fig. 14(b)]. The result is the gradually slowing spectral divergence of the soliton and radiation [Fig. 14(a)]. Physically, the frequency conversion of the radiation wave packet is due to the intrapulse four-wave mixing (see Sec. V), which is made possible by the sustained overlap of the radiation and soliton pulses.

Each of the solitons inside the supercontinuum shown in Figs. 2(b) and 11 has its own radiation pulse continuously drifting toward shorter wavelengths. We have found that the strongest soliton on the long-wavelength edge of the supercontinuum spectrum in Fig. 1(a) creates the potential V trapping around 20 modes on the short-wavelength edge. The radiation captured by the soliton can be represented as a superposition of these modes. Adiabatic transformation of the soliton power and width with propagation, caused by the increasing dispersion, induces weak adiabatic evolution of the mode parameters, but apart from this the modes are stationary solutions and hence their temporal and spectral dynamics are suppressed. Therefore approximating the radiation field as

$$F(z,\xi)=e^{-itgz/k_2''+g^2z^3/(3k_2'')}\sum_n\phi_n(\xi)e^{i\lambda_n z} \tag{20}$$

gives good matching with numerically computed spectral evolution of the short-wavelength edge of the supercontinuum (Gorbach and Skryabin, 2007b).

We would like to draw your attention to few points. First, the potential barrier (see Fig. 12) on the soliton side is high but still finite, so that some light leaks through it. The leaked radiation is especially noticeable in the higher-order modes [Figs. 2(b) and 12(c)]. Second, from numerical modeling of the supercontinuum it can be found that the rate of the soliton self-frequency shift on the red edge of the supercontinuum is actually higher

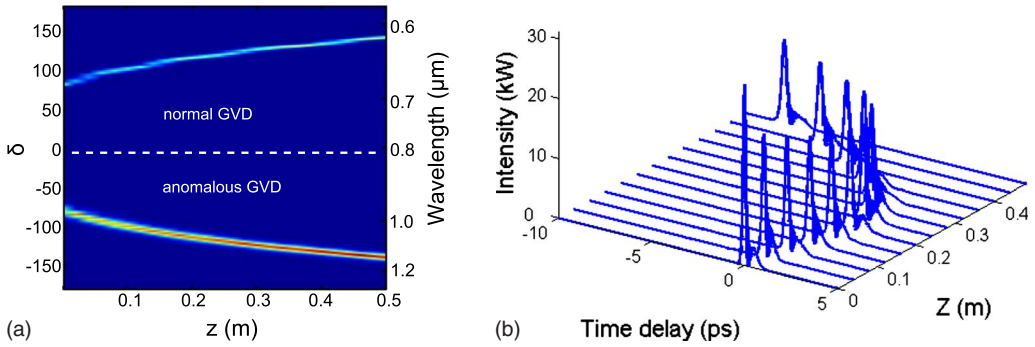

FIG. 14. (Color online) (a) Spectral and (b) time-domain evolutions of the soliton and trapped radiation modeled using the realistic frequency dependence of GVD [cf. (a) with Fig. 13]. (b) is plotted in the reference frame accelerating with g_0, which explains the curvature of the soliton trajectory opposite to the one in Fig. 5(a).

than for the bare soliton. Analytically this effect can be captured if g is calculated with nonlinear ϕ terms as accounted for by Gorbach and Skryabin (2007c). The resulting expression is $g=g_0(1+Pb^2)$. Here P is the peak power of radiation and b^2 is a constant. Third, to generate the spectra shown in Figs. 3, 11(a), and 11(c) we have used the same dispersion profiles and input powers but different input wavelengths. For Figs. 11(a) and 11(c) the pump was only 10 nm away from the zero GVD point; this has led to formation of less powerful solitons. Hence their frequency shift and the associated frequency shift of the short-wavelength radiation were substantially smaller leading to much narrower continua. Fourth, it has been reported that for high pump powers the solitons at the infrared edge of the continuum tend to collide and form bound states (Podlipensky *et al.*, 2008). These effects are naturally expected to influence radiation at the short-wavelength edge through the change of the trapping potential and collision-induced changes in soliton frequencies (Luan *et al.*, 2006).

It is important to note that the simultaneous and opposite soliton-radiation frequency conversion and radiation trapping have been observed in few experiments not related to the mainstream of the fiber supercontinuum research. The first we are aware of is the 1987 experiment by Beaud *et al.* (1987). Then there was a gap until 2001, when Nishizawa and Goto reported a series of spectral and time-domain measurements of the effect of pulse trapping by a soliton across the zero GVD point (Nishizawa and Goto, 2001, 2002). For recent experimental observations and frequency conversion applications of the trapping effect, see, e.g., Cumberland *et al.* (2008), Kudlinski and Mussot (2008), Stone and Knight (2008), Hill *et al.* (2009), and Nishizawa and Itoh (2009).

VII. GRAVITYLIKE EFFECTS, FREAK WAVES, AND TURBULENCE OF LIGHT IN FIBER

The parameter g used in Sec. VI has an obvious analogy with the acceleration of free fall. Equation (19) can be interpreted as the equation for a quantum particle in a gravity field and subject to the additional potential created by the soliton. If the radiation wave is prepared in such a way that it is both well localized in time and shifted away from the potential minimum, then it is a highly multimode state. Thus, according to the correspondence principle, one should expect quasiclassical dynamics to be seen. The wave packet should roll down a linear potential toward the soliton, reflect back from the latter, and, after some time, reconstruct itself in the original location. It is known though that the quasiclassical bouncing carries on only for limited time until it is replaced by the complete delocalization of the wave packet, which restores its shape again later. This effect is known as quantum bouncing (Robinett, 2004). Previously bouncing has been observed with clouds of Bose-condensed ultracold atoms subject to a gravity field and reflection of an atom mirror [see Bongs *et al.* (1999) and Saba *et al.* (1999) and Fig. 15(a)]. Figure 15(b) shows numerically modeled space-time evolution of the radiation pulse in the normal GVD range of an optical fiber bouncing on a decelerating soliton (Gorbach and Skryabin, 2007a). Similar light bouncing effects have also been reported for the curved waveguide arrays (Longhi,

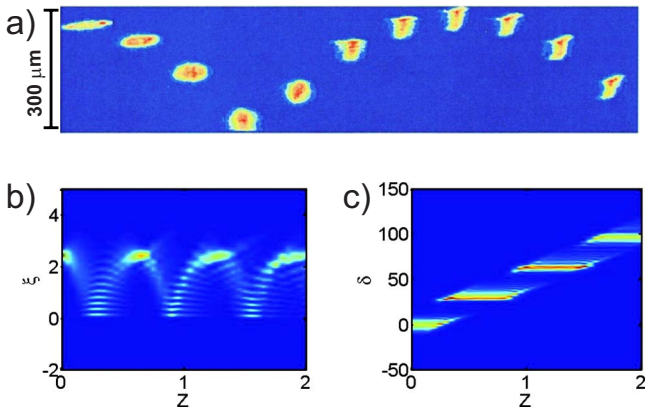

FIG. 15. (Color online) Bouncing of wave packets in linear potentials. (a) Series of images of the condensate bouncing off a light sheet (Bongs *et al.*, 1999). Time interval between the images is 2 ms along the horizontal axis. (b) Numerical modeling of the dispersive radiation bouncing off the decelerating soliton. ξ is the dimensionless time measured in the reference frame moving together with the soliton and z is the distance along the fiber. (c) Frequency δ conversion of the bouncing radiation (Gorbach and Skryabin, 2007a).

2008; Della Valle *et al.*, 2009). An important feature of our case is that on each reflection from the soliton the frequency of the radiation is up-shifted [see Fig. 15(c)]. Recently, the reflection of radiation from the soliton and the associated blueshift have been interpreted as the frequency shift at the white-hole horizon (Philbin *et al.*, 2008). The same work has predicted that the quantum effects of horizons, in particular Hawking radiation, can potentially be seen due to soliton-radiation interaction in optical fibers.

Another problem recently possessed by the supercontinuum and soliton research has been the question about the existence of optical freak or rogue waves (Solli *et al.*, 2007). This phenomenon has been actively studied in the context of ocean waves, where the rare waves, with probability not described by the tails of the Gaussian distribution, and the amplitude a few times larger than the average (for the current conditions) wave height possess serious and hardly predictable threat for ships and offshore industries. The NLS model is known to describe deep water waves including the freak events (Janssen, 2003). Therefore one can expect the appearance of similar phenomena in fiber optics. In particular, cases of the notable pulse to pulse fluctuations of the supercontinuum can be attributed to generation of the infrared solitons with unusually large amplitudes (Solli *et al.*, 2007, 2008; Dudley *et al.*, 2008). The probability for this to happen is described by the tail of the L-shaped distribution function. These freak solitons emerge essentially due to anomalously strong focusing developing in the course of modulational instability and the higher-order soliton fission (Solli *et al.*, 2007, 2008; Dudley *et al.*, 2008). There is also another class of localized freak wave solutions of NLS equation. These solutions are breathers, i.e., localized waves periodically absorbing and releasing their energy into the continuous wave background (Akhmediev and Wabnitz, 1992; Akhmediev *et al.*, 2009). This type of waves has the property of sudden appearance and disappearance, which is a known feature of the oceanic freak waves but still has not been seen in optical fibers.

Another area, where analogy between fluid mechanics and fiber optics is starting to produce interesting results, is turbulence research (Dyachenko *et al.*, 1992; Barviau *et al.*, 2008; Barviau, Kibler, and Picozzi, 2009). Spectral broadening due to multiple four-wave mixing processes of random weakly nonlinear waves can be associated with irreversible evolution of the spectrally narrow pump toward spectrally broad thermodynamic equilibrium (Barviau *et al.*, 2008; Barviau, Kibler, Kudlinski, *et al.*, 2009; Barviau, Kibler, and Picozzi, 2009). Current theoretical approaches to turbulence in general and to the turbulent supercontinuum have still not progressed to the level where the role of mixing of incoherent wave fields with coherent wave structures (solitons) in spectral broadening can be fully revealed (Dyachenko *et al.*, 1992). At the same time fiber supercontinuum research suggests that this difficult case is the most practically relevant. Complex "far from equilibrium" dynamics is also well known in fiber-based systems, such as fiber lasers and coherently pumped fiber resonators, where soliton pulses and spectral broadening often coexist [see, e.g., Mitschke *et al.* (1996), Lee *et al.* (2005), Babin *et al.* (2008), Peng *et al.* (2008), Chouli and Grelu (2009), and Kozyreff *et al.* (2009)].

VIII. SUMMARY

We summarize here those of the soliton properties which are most important for supercontinuum generation.

- Interaction of a soliton with dispersive radiation leads to the phase-matching sensitive generation of new frequencies. The most pronounced, out of few possible interaction channels, is the reflection of radiation from the refractive index change created by the soliton intensity. The reflection occurs provided the radiation frequency belongs to the normal GVD range. Depending on the sign of the third-order dispersion and the frequency of the incident radiation, the frequency of the reflected wave gets either up or down shifted.
- The Raman effect decelerates solitons and down shifts their frequency. Such solitons can interact with radiation repeatedly, trap it on the time scales of 100 fs, and continuously up shift the radiation frequency.

The prevalent scenario of the supercontinuum generation in photonic-crystal fibers pumped by femtosecond pulses with the input wavelength around the zero GVD point can be summarized as follows:

- The spectrum of the input pulse is distributed in some proportion between the frequency ranges with normal and anomalous GVDs. This occurs through the combination of nonlinear processes. SPM dominates during the first few centimeters of propagation. Then the soliton fission accompanied by the radiation emission and reflection of the dispersive waves from emerging solitons lead to further spectral broadening.
- The next stage is when the Raman shifted solitons on the long-wavelength edge of the supercontinuum enter into the regime of the cascaded interaction with dispersive radiation. This quickly leads to the formation of the bound soliton-radiation states responsible for continuous spectral divergence of the supercontinuum edges. The necessary condition for this to occur is the near matching of the group velocities across the zero GVD point.

Using nanosecond or cw pump for supercontinuum generation leads to modulational instability and subsequent creation of a soliton train. The latter trap radiation and the above scenario are realized again albeit with a greater number of solitons (Cumberland *et al.*, 2008; Kudlinski and Mussot, 2008; Stone and Knight, 2008; Travers, 2009) and a greater sensitivity to noise (Solli *et al.*, 2007; Turitsyn and Derevyanko, 2008).

IX. PERSPECTIVES

The interaction between solitons and radiation, optical turbulence, freak waves, and the development of ideas around the gravitylike forces exerted on light by solitons are all on the list of problems stimulated by the fiber supercontinuum research and undergoing the stage of active exploration. Supercontinuum generation has been of course known outside the fiber context in bulk solids, liquids, and gases [see, e.g., Bergé *et al.* (2007), Couairon and Mysyrowicz (2007), Kolesik and Moloney (2008)], where all three space dimensions are important. The role of spatial and spatiotemporal solitons in these systems is still far from been fully explored (Yulin *et al.*, 2005; Bergé *et al.*, 2007). The generation of broad spatial and frequency spectra in nonlinear photonic crystals is another area where the interaction of solitons with diffracting and dispersing waves can be important (Bartal *et al.*, 2006; Manela *et al.*, 2006; Babushkin *et al.*, 2007; Jia *et al.*, 2007; Benton *et al.*, 2008; Dong *et al.*, 2008). Strong field localization in metallic optical nanoantennas has been demonstrated to lead to supercontinuum generation (Muhlschlegel *et al.*, 2005), thereby linking the effects discussed above with nanophotonics. A possibility of nonlinear optical processes in nature made optical waveguides, e.g., found in sea organisms and sometimes having a structure of fibers with few micron core diameters and photonic-crystal cladding (Aizenberg *et al.*, 2004; Kulchin *et al.*, 2008), remain an intriguing problem to consider. Overall, a bidirectional flow of ideas between fiber photonics and other branches of optics and physics in general is more than likely to stimulate further progress in the soliton and supercontinuum related research.

REFERENCES

Afanasjev, V. V., Y. S. Kivshar, and C. R. Menyuk, 1996, Opt. Lett. **21**, 1975.

Agrawal, G., 2007, *Nonlinear Fiber Optics* (Academic, New York).

Aizenberg, J., V. C. Sundar, A. D. Yablon, J. C. Weaver, and G. Chen, 2004, Proc. Natl. Acad. Sci. U.S.A. **101**, 3358.

Akhmediev, N., A. Ankiewicz, and M. Taki, 2009, Phys. Lett. A **373**, 675.

Akhmediev, N., and M. Karlsson, 1995, Phys. Rev. A **51**, 2602.

Akhmediev, N., W. Krolikowski, and A. Lowery, 1996, Opt. Commun. **131**, 260.

Akhmediev, N. N., and S. Wabnitz, 1992, J. Opt. Soc. Am. B **9**, 236.

Amiranashvili, S., A. G. Vladimirov, and U. Bandelow, 2008, Phys. Rev. A **77**, 063821.

Babin, S. A., V. Karalekas, E. V. Podivilov, V. K. Mezentsev, P. Harper, J. D. Ania-Castanon, and S. K. Turitsyn, 2008, Phys. Rev. A **77**, 033803.

Babushkin, I., A. Husakou, J. Herrmann, and Y. S. Kivshar, 2007, Opt. Express **15**, 11978.

Bartal, G., O. Manela, and M. Segev, 2006, Phys. Rev. Lett. **97**, 073906.

Barviau, B., B. Kibler, S. Coen, and A. Picozzi, 2008, Opt. Lett. **33**, 2833.

Barviau, B., B. Kibler, A. Kudlinski, A. Mussot, G. Millot, and A. Picozzi, 2009, Opt. Express **17**, 7392.

Barviau, B., B. Kibler, and A. Picozzi, 2009, Phys. Rev. A **79**, 063840.

Beaud, P., W. Hodel, B. Zysset, and H. Weber, 1987, IEEE J. Quantum Electron. **23**, 1938.

Benton, C. J., A. V. Gorbach, and D. V. Skryabin, 2008, Phys. Rev. A **78**, 033818.

Bergé, L., S. Skupin, R. Nuter, J. Kasparian, and J. P. Wolf, 2007, Rep. Prog. Phys. **70**, 1633.

Biancalana, F., D. V. Skryabin, and A. V. Yulin, 2004, Phys. Rev. E **70**, 016615.

Bongs, K., S. Burger, G. Birkl, K. Sengstock, W. Ertmer, K. Rzazewski, A. Sanpera, and M. Lewenstein, 1999, Phys. Rev. Lett. **83**, 3577.

Chouli, S., and P. Grelu, 2009, Opt. Express **17**, 11776.

Corwin, K. L., N. R. Newbury, J. M. Dudley, S. Coen, S. A. Diddams, K. Weber, and R. S. Windeler, 2003, Phys. Rev. Lett. **90**, 113904.

Couairon, A., and A. Mysyrowicz, 2007, Phys. Rep. **441**, 47.

Cristiani, I., R. Tediosi, L. Tartara, and V. Degiorgio, 2004, Opt. Express **12**, 124.

Cumberland, B. A., J. C. Travers, S. V. Popov, and J. R. Taylor, 2008, Opt. Lett. **33**, 2122.

Della Valle, G., M. Savoini, M. Ornigotti, P. Laporta, V. Foglietti, M. Finazzi, L. Duo, and S. Longhi, 2009, Phys. Rev. Lett. **102**, 180402.

Dong, R., C. E. Ruter, D. Kip, O. Manela, M. Segev, C. L. Yang, and J. J. Xu, 2008, Phys. Rev. Lett. **101**, 183903.

Dudley, J. M., and S. Coen, 2002, Opt. Lett. **27**, 1180.

Dudley, J. M., G. Genty, and S. Coen, 2006, Rev. Mod. Phys. **78**, 1135.

Dudley, J. M., G. Genty, and B. J. Eggleton, 2008, Opt. Express **16**, 3644.

Dudley, J. M., and J. R. Taylor, 2009, Nat. Photonics **3**, 85.

Dyachenko, S., A. C. Newell, A. Pushkarev, and V. E. Zakharov, 1992, Physica D **57**, 96.

Efimov, A., A. J. Taylor, F. G. Omenetto, A. V. Yulin, N. Y. Joly, F. Biancalana, D. V. Skryabin, J. C. Knight, and P. S. Russell, 2004, Opt. Express **12**, 6498.

Efimov, A., A. J. Taylor, A. V. Yulin, D. V. Skryabin, and J. C. Knight, 2006, Opt. Lett. **31**, 1624.

Efimov, A., A. V. Yulin, D. V. Skryabin, J. C. Knight, N. Joly, F. G. Omenetto, A. J. Taylor, and P. Russell, 2005, Phys. Rev. Lett. **95**, 213902.

Falk, P., M. H. Frosz, and O. Bang, 2005, Opt. Express **13**, 7535.

Frosz, M. H., P. Falk, and O. Bang, 2005, Opt. Express **13**, 6181.

Gagnon, L., and P. A. Belanger, 1990, Opt. Lett. **15**, 466.

Genty, G., M. Lehtonen, and H. Ludvigsen, 2004, Opt. Express **12**, 4614.

Genty, G., M. Lehtonen, and H. Ludvigsen, 2005, Opt. Lett. **30**, 756.

Genty, G., M. Lehtonen, H. Ludvigsen, and M. Kaivola, 2004, Opt. Express **12**, 3471.

Gorbach, A., D. Skryabin, J. Stone, and J. Knight, 2006, Opt. Express **14**, 9854.

Gorbach, A. V., and D. V. Skryabin, 2007a, Opt. Express **15**, 14560.

Gorbach, A. V., and D. V. Skryabin, 2007b, Nat. Photonics **1**, 653.

Gorbach, A. V., and D. V. Skryabin, 2007c, Phys. Rev. A **76**,

053803.
Gorbach, A. V., and D. V. Skryabin, 2008, Opt. Express **16**, 4858.
Gorshkov, K. A., and L. A. Ostrovsky, 1981, Physica D **3**, 428.
Gu, X., M. Kimmel, A. P. Shreenath, R. Trebino, J. M. Dudley, S. Coen, and R. S. Windeler, 2003, Opt. Express **11**, 2697.
Harbold, J. M., F. O. Ilday, F. W. Wise, T. A. Birks, W. J. Wadsworth, and Z. Chen, 2002, Opt. Lett. **27**, 1558.
Hasegawa, A., and F. Tappert, 1973, Appl. Phys. Lett. **23**, 142.
Herrmann, J., U. Griebner, N. Zhavoronkov, A. Husakou, D. Nickel, J. C. Knight, W. J. Wadsworth, P. S. J. Russell, and G. Korn, 2002, Phys. Rev. Lett. **88**, 173901.
Hill, S., C. E. Kuklewicz, U. Leonhardt, and F. König, 2009, Opt. Express **17**, 13588.
Hori, T., N. Nishizawa, T. Goto, and M. Yoshida, 2004, J. Opt. Soc. Am. B **21**, 1969.
Husakou, A. V., and J. Herrmann, 2001, Phys. Rev. Lett. **87**, 203901.
Janssen, P. A. E. M., 2003, J. Phys. Oceanogr. **33**, 863.
Jia, S., W. Wan, and J. W. Fleischer, 2007, Phys. Rev. Lett. **99**, 223901.
Karpman, V. I., 1993a, Phys. Rev. E **47**, 2073.
Karpman, V. I., 1993b, Phys. Lett. A **181**, 211.
Kaup, D. J., and A. C. Newell, 1978, Proc. R. Soc. London, Ser. A **361**, 413.
Kivshar, Y. S., and B. A. Malomed, 1989, Rev. Mod. Phys. **61**, 763.
Knight, J. C., and D. V. Skryabin, 2007, Opt. Express **15**, 15365.
Kolesik, M., and J. V. Moloney, 2008, Opt. Express **16**, 2971.
Kozyreff, G., M. Tlidi, A. Mussot, E. Louvergneaux, M. Taki, and A. G. Vladimirov, 2009, Phys. Rev. Lett. **102**, 043905.
Kudlinski, A., and A. Mussot, 2008, Opt. Lett. **33**, 2407.
Kulchin, Y. N., S. N. Bagaev, O. A. Bukin, S. S. Voznesenskii, A. L. Drozdov, Y. A. Zinin, I. G. Nagornyi, E. V. Pestryakov, and V. I. Trunov, 2008, Tech. Phys. Lett. **34**, 633.
Kuznetsov, E. A., A. V. Mikhailov, and I. A. Shimokhin, 1995, Physica D **87**, 201.
Lee, J., Y. Takushinia, and K. Kikuchi, 2005, Opt. Lett. **30**, 2599.
Longhi, S., 2008, Phys. Rev. A **77**, 035802.
Luan, F., D. Skryabin, A. Yulin, and J. Knight, 2006, Opt. Express **14**, 9844.
Manela, O., G. Bartal, M. Segev, and H. Buljan, 2006, Opt. Lett. **31**, 2320.
Milián, C., D. V. Skryabin, and A. Ferrando, 2009, Opt. Lett. **34**, 2096.
Mitschke, F., and L. Mollenauer, 1986, Opt. Lett. **11**, 659.
Mitschke, F., G. Steinmeyer, and A. Schwache, 1996, Physica D **96**, 251.
Mollenauer, L., and J. Gordon, 2006, *Solitons in Optical Fibers: Fundamentals and Applications* (Academic, New York).
Mollenauer, L. F., R. H. Stolen, and J. P. Gordon, 1980, Phys. Rev. Lett. **45**, 1095.
Muhlschlegel, P., H. J. Eisler, O. J. F. Martin, B. Hecht, and D. W. Pohl, 2005, Science **308**, 1607.
Nishizawa, N., and T. Goto, 2001, Opt. Express **8**, 328.
Nishizawa, N., and T. Goto, 2002, Opt. Express **10**, 1151.
Nishizawa, N., and K. Itoh, 2009, Appl. Phys. Express **2**, 062501.
Peng, J., F. Zhu, and A. V. Sokolov, 2008, Opt. Lett. **33**, 1620.
Philbin, T. G., C. Kuklewicz, S. Robertson, S. Hill, F. Konig, and U. Leonhardt, 2008, Science **319**, 1367.
Podlipensky, A., P. Szarniak, N. Y. Joly, and P. S. J. Russell, 2008, J. Opt. Soc. Am. B **25**, 2049.
Ranka, J. K., R. S. Windeler, and A. J. Stentz, 2000, Opt. Lett. **25**, 25.
Robinett, R. W., 2004, Phys. Rep. **392**, 1.
Russell, P. S. J., 2006, J. Lightwave Technol. **24**, 4729.
Saba, C. V., P. A. Barton, M. G. Boshier, I. G. Hughes, P. Rosenbusch, B. E. Sauer, and E. A. Hinds, 1999, Phys. Rev. Lett. **82**, 468.
Scott, A., 1999, *Nonlinear Science: Emergence and Dynamics of Coherent Structures* (Oxford University Press, Oxford).
Skryabin, D. V., F. Luan, J. C. Knight, and P. S. Russell, 2003, Science **301**, 1705.
Skryabin, D. V., and A. V. Yulin, 2005, Phys. Rev. E **72**, 016619.
Solli, D. R., C. Ropers, and B. Jalali, 2008, Phys. Rev. Lett. **101**, 233902.
Solli, D. R., C. Ropers, P. Koonath, and B. Jalali, 2007, Nature (London) **450**, 1054.
Stone, J. M., and J. C. Knight, 2008, Opt. Express **16**, 2670.
Travers, J., 2009, Opt. Express **17**, 1502.
Travers, J. C., and J. R. Taylor, 2009, Opt. Lett. **34**, 115.
Tsoy, E., and C. M. deSterke, 2006, J. Opt. Soc. Am. B **23**, 2425.
Turitsyn, S. K., and S. A. Derevyanko, 2008, Phys. Rev. A **78**, 063819.
Wadsworth, W. J., A. Ortigosa-Blanch, J. C. Knight, T. A. Birks, T. P. M. Man, and P. S. Russell, 2002, J. Opt. Soc. Am. B **19**, 2148.
Wai, P. K. A., H. H. Chen, and Y. C. Lee, 1990, Phys. Rev. A **41**, 426.
Yulin, A. V., D. V. Skryabin, and P. S. J. Russell, 2004, Opt. Lett. **29**, 2411.
Yulin, A. V., D. V. Skryabin, and P. S. J. Russell, 2005, Opt. Lett. **30**, 525.
Zakharov, V. E., and A. B. Shabat, 1972, Sov. Phys. JETP **34**, 62.